Supporting Information

Nisemblat et al. 10.1073/pnas.1411718112

SI Materials and Methods

Protein Preparation. mHsp60^{E321K} mutant was cloned and purified as previously reported (1). In this construct, the 17 amino acids of the C terminus tail that include the GGM repeats, which are predicted to be unstructured, were removed during the cloning process. GroEL and GroES were purified as described by Bonshtien et al. (2). WT mHsp60 was purified as described by Parnas et al. (3). The 6× His-tag GroES was purified as described by Zondlo et al. (4), with slight changes in the last step when the buffer was changed to 10 mM Tris·HCl (pH 7.5) and 200 mM NaCl using a PD-10 desalting column (GE Healthcare).

Human Hsp10 (mHsp10) cDNA (GenBank accession no. P61604) was inserted into the pET22b(+) expression plasmid (Novagen) using NdeI and XhoI restriction sites. A stop codon was inserted at the end of the cDNA sequence to generate a construct that does not contain a C terminus His-tag. An mHsp10 construct containing a C-terminal 6× His-tag, separated by a seven-amino acid linker, was generated by insertion of mHsp10 cDNA into the pET22b(+) plasmid via the NdeI and HindIII restriction sites. His-tagged mHsp10 was expressed and purified as described by Dickson et al. (5) and Parnas et al. (6). The non–His-tagged mHsp10 was expressed, as was the His-tagged mHsp10. This construct was purified as follows. The cell pellet was resuspended (1:10 wt/vol) in a buffer containing 20 mM Tris·HCl (pH 7.7), 5 mM $MgSO_4$, 1 mM DTT, and 1,500 units of DNase. Cells were homogenized and passed through a microfluidizer. Immediately after lysis, PMSF (0.5 mM) and the following protease inhibitors (1 μg/mL each; Sigma) were added: pepstatin, chymostatin, antipain, leupeptin, and aprotinin. Debris was removed by centrifugation for 30 min at 35,000 × *g*. The supernatant was loaded onto a RESOURCE Q column (GH Healthcare) equilibrated with buffer A [20 mM Tris·HCl (pH 7.7), 0.1 mM EDTA, and 1 mM DTT]. Unbound proteins were collected from the column and dialyzed overnight against buffer B [20 mM MES (pH 6.6) and 0.1 mM EDTA]. The protein was then loaded on a SOURCE-S column (GH Healthcare) equilibrated with buffer B. Bound proteins were eluted from the column with a linear gradient of 0–500 mM NaCl (in buffer B). The mHsp10-enriched fractions were collected and concentrated. The protein was then loaded on a Superdex 200 prep grade gel-filtration column (Pharmacia) equilibrated with buffer C [50 mM Tris·HCl (pH 7.7) and 100 mM NaCl]. Fractions containing heptameric mHsp10 were concentrated to ∼30–40 mg/mL and flash-frozen in liquid nitrogen for storage. All stages were carried out at 4 °C. On average, ∼15 mg of mHsp10 per gram of cell pellet was obtained.

SeM–mHsp60^{E321K} was overexpressed and purified as above, with the slight changes needed to inhibit the methionine pathway (7, 8).

mHsp60 triple mutant (mHsp60^{TM}), harboring E105A, K109Q, and E462A mutations, was cloned and purified as for the WT mHsp60 (mutant gene was purchased from Syntezza Bioscience). In the last purification step (oligomerization of the complex), about 80% of the protein aggregated, and after size exclusion chromatography (Superdex 200 prep grade; Pharmacia), only ∼10% of the protein (7 mg) remained.

EGFP cDNA was amplified by using the following primers:

Forward EGFP: CCTGTATTTTCAGGGCGGGCGCGCCATGGTGAGCAAGGGCGAGGAGCTGTTCACC

Reverse EGFP: CATTATGCGGCCGCAAGCTTGTCGACTTACTTGTACAGCTCGTCCATGCCGAGAGTGATCC

Using the above primers and the Gibson method (New England Biolabs), the cDNA was inserted into the pCDFDuet plasmid (Novagen) downstream to an N terminus 6× His-tag, followed by the maltose-binding protein (MBP) sequence and a tobacco etch virus (TEV) protease digestion site. The plasmid was transformed into BL21 bacteria, and the EGFP-fused MBP protein was overexpressed by induction with 1 mM isopropyl-β-D-thiogalactopyranoside (IPTG) and grown at 30 °C for 4 h. The cells were resuspended (1:10 wt/vol) in buffer A [50 mM Tris·HCl (pH 7.7), 100 mM NaCl, and 5 mM imidazole], supplemented with 1,500 units of DNase, 0.5 mM PMSF, and a 1/1,000 dilution of protease inhibitor mixture set III EDTA-free (Calbiochem). Cells were homogenized and disrupted by sonication. Debris was removed by centrifugation for 30 min at 35,000 × *g*. The supernatant was loaded onto a nickel-agarose resin column equilibrated with buffer B [20 mM Tris·HCl (pH 7.7), 300 mM NaCl, and 20 mM imidazole]. Bound proteins were eluted with buffer B containing 250 mM imidazole. To remove the fused MBP, a His-tagged TEV protease was added at a ratio of 1:30 (wt/wt). The protein sample was then dialyzed overnight against 2 L of buffer B lacking imidazole. Next, the protein was loaded again onto a nickel-agarose resin column that was equilibrated with buffer B, and the unbound EGFP protein was collected. At the final stage, the buffer was exchanged to buffer C [20 mM Tris·HCl (pH 7.7) and 300 mM NaCl] using a PD-10 desalting column (GE Healthcare). Fractions containing EGFP were concentrated to ∼35–40 mg/mL and flash-frozen in liquid nitrogen for storage. All purification steps were carried out at 4 °C. We obtained ∼55 mg of EGFP per 10 g of cell pellet.

Packing Arrangement of the mHsp60^{E321K}–mHsp10 Complex. The mHsp60^{E321K}–mHsp10 complex crystallized in the space group $P4_12_12$ with cell dimensions of $a = b$ =199.10 Å, c = 627.39 Å. The asymmetric unit of the structure contains the full football model [i.e., $mHsp60_{14}$–$(mHsp10_7)_2$ complex]. The long axis of the complex closely coincides with the long axis of the unit cell, with a deviation of about 3° along a diagonal of the *a*/*b* cell face. One complex makes packing contacts with 12 symmetry-related complexes: four in the central plane of the complex (Fig. S5*A*) and eight touching the north and south parts of the football.

Among the interactions that exist between the 12 symmetry-related football complexes, one is of extreme significance to the successful crystallization of the complex. The protruding His-tag of subunit Z of mHsp10 makes contact with subunits F and G of mHsp60 of one of the neighboring footballs (Fig. S5*B*; the nomenclature for subunits is shown in Fig. S4). Only one interaction of this type can be formed and only in the south ringed mHsp10, owing to the interplay of the sevenfold NCS of the football particle and the fourfold symmetry of the crystal. The next neighboring symmetric molecule will be 90° (360°/4) apart from the first one, but the closest His-tag will be 102.8° (360°/7 × 2) apart.

Additional interesting interactions observed within the 12 symmetry-related football complexes include one in which the apical domain of subunits G and N are stabilized by interaction with subunits of the neighboring symmetry-related footballs. The apical domain of subunit G interacts with subunits L, M, Z, and 1 of the neighboring football, while the apical domain of subunit N interacts with subunits J, K, and Y of a different neighboring football (Fig. S5 *C* and *D*). These two lattice contact points stabilize the new conformation of subunits G and N, which present ∼100° counterclockwise rotation compared with the other apical domains in the ring.

In Vitro Activity Experiments. Refolding of HCl-denatured malate dehydrogenase was carried out as previously described (9).

SEC-MALS Experiments. Different chaperonins (WT mHsp60, mHsp60^{E321K}, mHsp60, or GroEL) were diluted to 50 μM in buffer containing 20 mM Tris·HCl (pH 7.7), 10 mM $MgCl_2$, 20 mM KCl, and 2 mM ATP (when indicated). In some of the experiments, 50 μM His-tagged mHsp10 or 50 μM nontagged mHsp10 was added to the reaction mixture. After incubation for 5 min at room temperature (~25 °C), the proteins were injected into an SEC column (SRT SEC-500; Sepax Technologies) that was equilibrated with the same buffer. The column was connected to a MALS detector (DAWN HELEOS II; Wyatt Technology) and then to a refractive index detector (Optilab t-rEX; Wyatt Technology). Wyatt Astra V software was used for data collection and analysis. Data were collected at ~25 °C.

EGFP Experiments.

EGFP refolding experiments. Purified EGFP (350 μg) was denatured by incubation with 100 mM HCl for 5 min. Binary complex (700 μL) was formed by mixing 4 μM denatured EGFP with 60 μM different chaperonins (as indicated) in buffer A [20 mM Tris·HCl (pH 7.7), 10 mM $MgCl_2$, 1 mM KCl, and 5 mM DTT] and incubation for 5 min at room temperature (RT). After incubation, the refolding reaction was induced by adding a 350-μL mix of 240 μM cochaperonin and 3 mM ATP in buffer A and further incubation for 5 min (final ratio of chaperonin/cochaperonin was 1:2). Then, the samples were injected into a Superdex 75 prep grade gel-filtration column (Pharmacia) equilibrated with buffer A (supplemented with 1 mM ATP). Fraction fluorescence was measured using a SynergyHT plate reader (Biotek) with a 485/20 excitation filter, a 528/20 emission filter, and a gain of 55. In addition, samples from the fractions were run on 14% (wt/vol) SDS-PAGE.

EGFP pull-down experiments. Denatured EGFP was obtained as above. This time, a 140-μL binary complex was formed by mixing 1 μM denatured EGFP with 15 μM different chaperonins (as indicated) in buffer B [20 mM Tris·HCl (pH 7.7), 10 mM $MgCl_2$, 1 mM KCl, and 20 mM imidazole], followed by 5 min of incubation at RT. Next, 70 μL of His-tagged cochaperonin-nucleotide mix (60 μM cochaperonin) was added to the binary complex and incubated for 5 min. Then, the samples were incubated for 10 min with 40 μL of nickel-nitrilotriacetic acid beads (GE Healthcare) on an end-to-end shaker at RT. Samples were centrifuged and washed three times with 210 μL of buffer B containing 0.5 mM nucleotide (as indicated). The last wash was carried out with buffer B lacking imidazole. Pellets containing Ni beads and bound proteins were then resuspended with 210 μL of buffer B (without imidazole), and their fluorescence was measured as described above.

Interactions Between Amino Acid Residues. Interactions between amino acid residues in the mHsp60–mHsp10 structure were calculated using the Protein Interactions Calculator server (10) and the PISA server (11). The latter was also used for calculations of surface contact areas.

The rmsd values between different subunits in the structure (Tables S2 and S3) were calculated using the DaliLite program at the European Bioinformatics Institute web server (12).

Graphics Packages for Rendering of Figures. Figures were generated using the UCSF Chimera package (13) or the PyMOL program (The PyMOL Molecular Graphics System, version 1.5.0.4; Schrödinger, LLC; available at www.pymol.org).

1. Nisemblat S, Parnas A, Yaniv O, Azem A, Frolow F (2014) Crystallization and structure determination of a symmetrical 'football' complex of the mammalian mitochondrial Hsp60-Hsp10 chaperonins. *Acta Crystallogr F Struct Biol Commun* 70(Pt 1):116–119.
2. Bonshtien AL, et al. (2007) Significance of the N-terminal domain for the function of chloroplast cpn20 chaperonin. *J Biol Chem* 282(7):4463–4469.
3. Parnas A, et al. (2012) Identification of elements that dictate the specificity of mitochondrial Hsp60 for its co-chaperonin. *PLoS ONE* 7(12):e50318.
4. Zondlo J, Fisher KE, Lin Z, Ducote KR, Eisenstein E (1995) Monomer-heptamer equilibrium of the Escherichia coli chaperonin GroES. *Biochemistry* 34(33):10334–10339.
5. Dickson R, et al. (1994) Cloning, expression, and purification of a functional non-acetylated mammalian mitochondrial chaperonin 10. *J Biol Chem* 269(43):26858–26864.
6. Parnas A, et al. (2009) The MitCHAP-60 disease is due to entropic destabilization of the human mitochondrial Hsp60 oligomer. *J Biol Chem* 284(41):28198–28203.
7. Van Duyne GD, Standaert RF, Karplus PA, Schreiber SL, Clardy J (1993) Atomic structures of the human immunophilin FKBP-12 complexes with FK506 and rapamycin. *J Mol Biol* 229(1):105–124.
8. Opatowsky Y, et al. (2006) Structure-function studies of the G-domain from human gem, a novel small G-protein. *FEBS Lett* 580(25):5959–5964.
9. Bonshtien AL, et al. (2009) Differential effects of co-chaperonin homologs on cpn60 oligomers. *Cell Stress Chaperones* 14(5):509–519.
10. Tina KG, Bhadra R, Srinivasan N (2007) *PIC: Protein Interactions Calculator. Nucleic Acids Res* 35(Web Server issue):W473–W476.
11. Krissinel E, Henrick K (2007) Inference of macromolecular assemblies from crystalline state. *J Mol Biol* 372(3):774–797.
12. Holm L, Park J (2000) DaliLite workbench for protein structure comparison. *Bioinformatics* 16(6):566–567.
13. Pettersen EF, et al. (2004) UCSF Chimera—A visualization system for exploratory research and analysis. *J Comput Chem* 25(13):1605–1612.

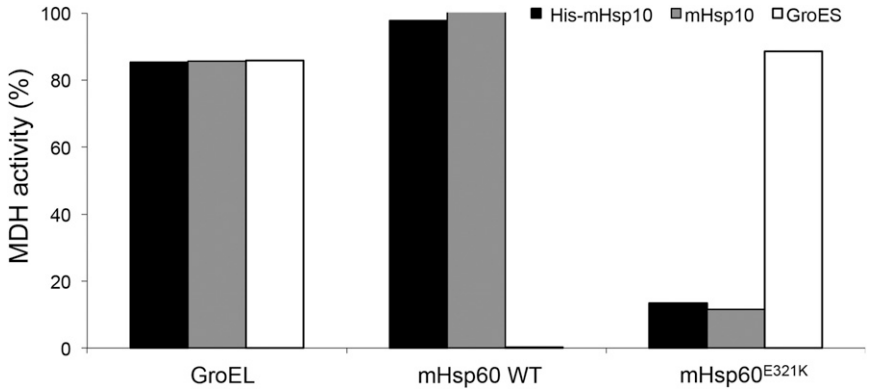

Fig. S1. mHsp60^{E321K} mutation switches its cochaperonin specificity. Refolding of 0.33 μM HCl-denatured malate dehydrogenase (MDH) by the indicated chaperonin (10 μM) and 20 μM His-mHsp10 (black columns), mHsp10 (gray column), or GroES (white columns). MDH activity was measured at 340 nm after incubation for 60 min at 30 °C in the presence of 1 mM ATP. The refolding activity is presented relative to the refolding activity of native MDH (100%).

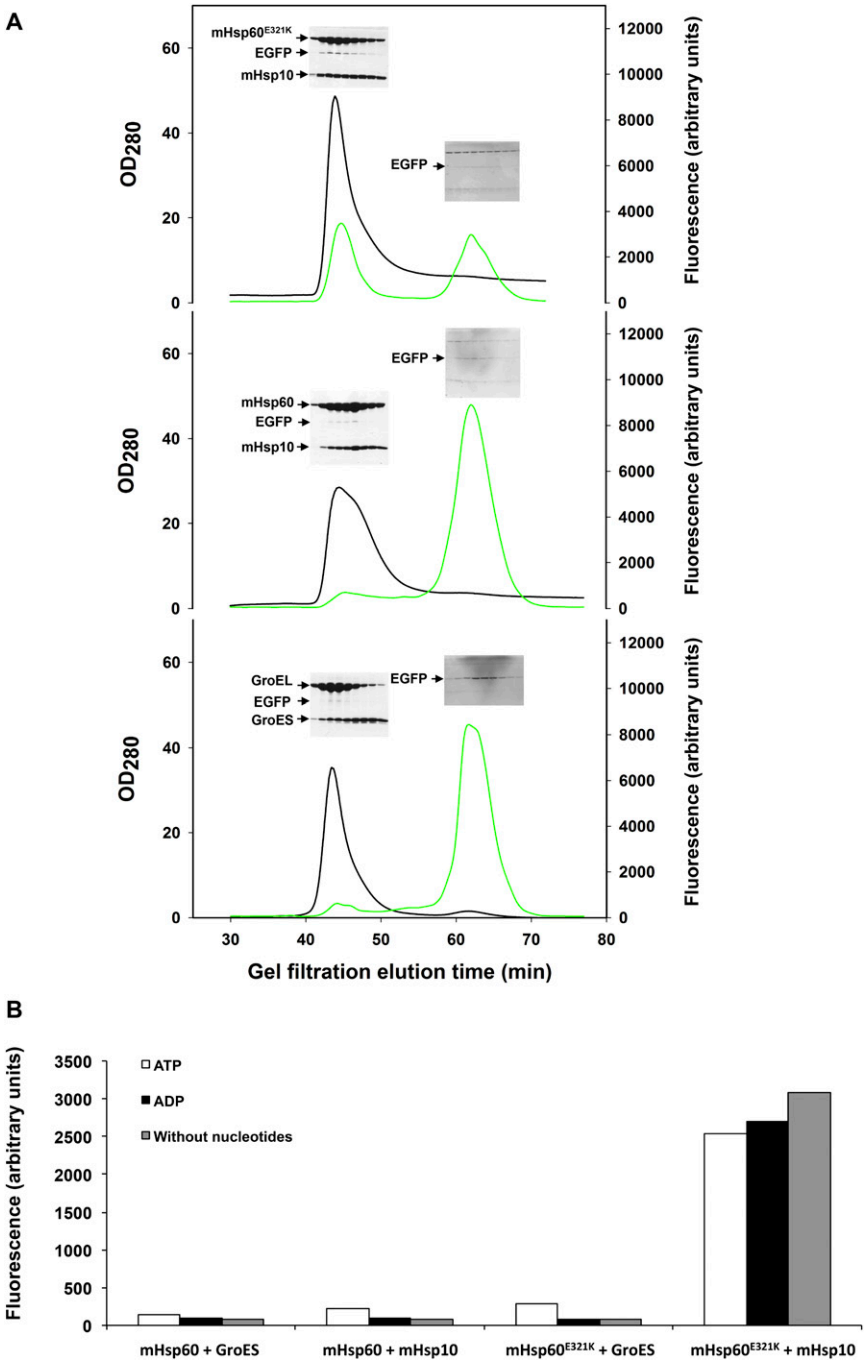

Fig. S2. mHsp60^{E321K} can encapsulate and refold EGFP. (*A*) Size exclusion chromatography of mHsp60^{E321K} + mHsp10 (*Top*), mHsp60 + mHsp10 (*Middle*), and GroEL + GroES (*Lower*) complexed to unfolded EGFP. Each chaperonin (40 μM) was incubated with 2.5 μM HCl-denatured EGFP. After addition of the indicated cochaperonin (80 μM) and 1 mM ATP, the samples were loaded on a Superdex 75 prep grade column and the OD at 280 nm (black line) and EGFP fluorescence (green line) were monitored. Samples from the peak areas were run on 14% (wt/vol) SDS-PAGE (gel images above each peak). Because the interaction of the mHsp60–mHsp10 complex and GroEL/GroES is dynamic, the refolded EGFP is eluted as "free" EGFP after the chaperonin peak. In contrast, when EGFP is complexed to the mHsp60^{E321K}–mHsp10 stuck complex, ~50% of the folded EGFP elutes as "trapped" EGFP (stuck inside the mHsp60^{E321K}–mHsp10 complex cavity). (*B*) Pull-down experiments with His-tagged cochaperonins. mHsp60 or mHsp60^{E321K} (10 μM), together with 1 μM HCl-denatured EGFP and 20 μM His-tagged GroES or His-tagged mHsp10, was incubated with nickel beads in the presence of 1 mM ATP (white columns), 1 mM ADP (black columns), or no nucleotide (gray columns). After washing, the beads were resuspended in buffer and the EGFP fluorescence was measured. Similar to the results in *A*, the mHsp60–mHsp10 and mHsp60^{E321K}–GroES complexes are dynamic, such that the folded EGFP is eliminated during the washing steps. Because GroES does not bind mHsp60, no pull-down occurs in this sample. As before, the mHsp60^{E321K}–mHsp10 stuck complex is the only one able to trap folded EGFP, even in the presence of ADP or in the absence of nucleotide (the mHsp60^{E321K} mutant is stabilized in the "open" conformation, the form adopted in the presence of ATP).

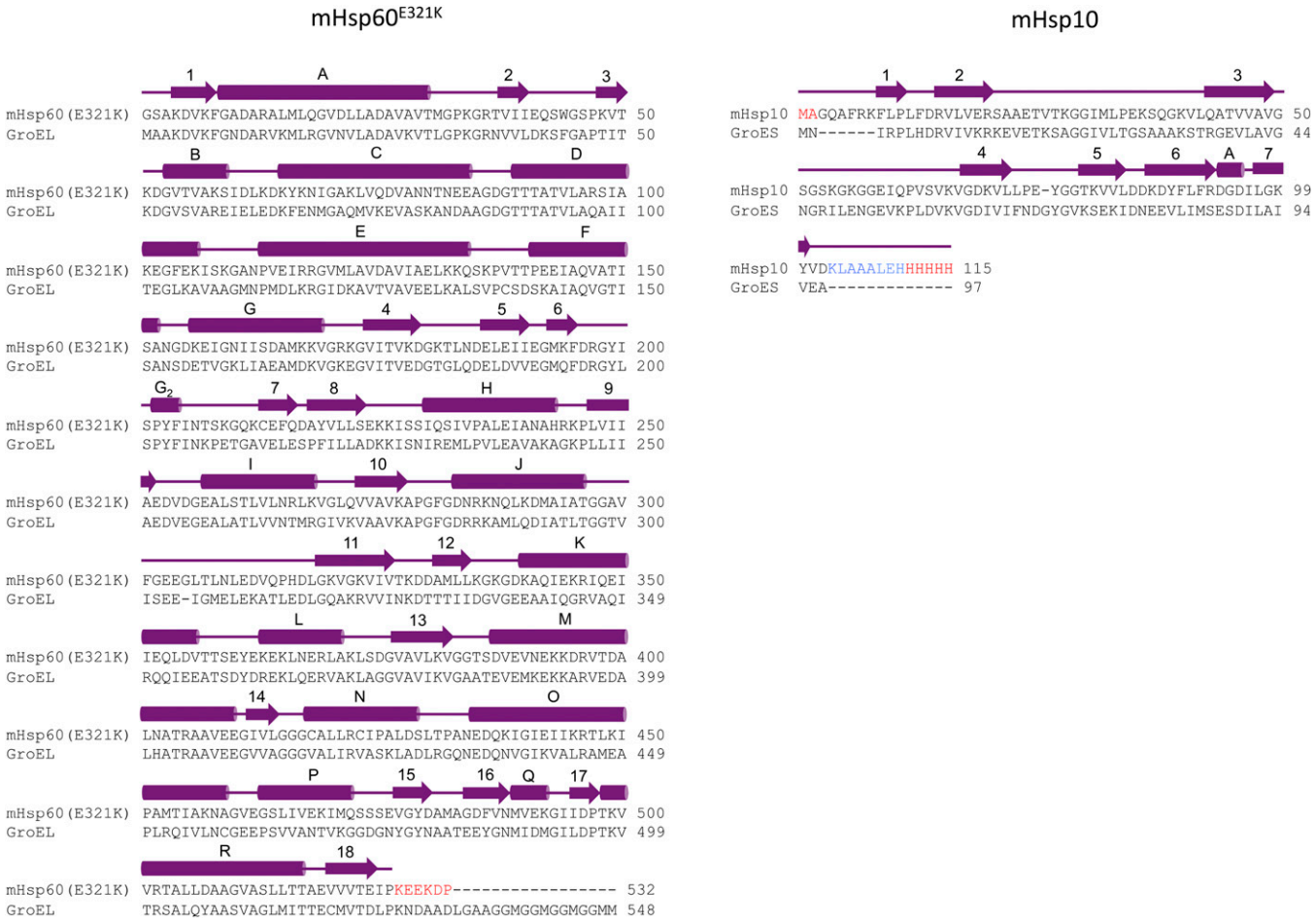

Fig. S3. Diagram of the secondary structure of mHsp60^{E321K} and mHsp10. Elements of the secondary structure of chains A (representative of all mHsp60^{E321K} subunits) and O (representative of all mHsp10 subunits) are indicated above the amino acid sequence alignment of mHsp60^{E321K} and GroEL or mHsp10 and GroES. Numbered arrows indicate β-sheets, and alphabetically marked cylinders represent α-helices. Blue letters indicate residues for which electron densities were observed in only part of the chains, whereas red letters indicate residues for which electron densities were not observed. The 17-aa tail at the C-terminal end of the mHsp60 protein, which is predicted to be unstructured, was removed during the mHsp60^{E321K} cloning process.

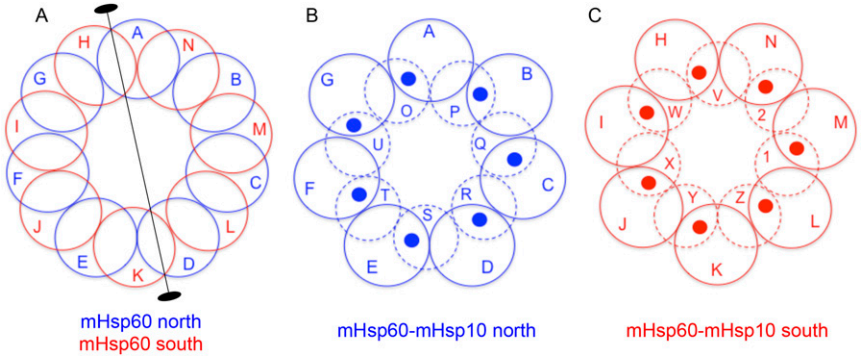

Fig. S4. Architecture and nomenclature of subunits in the $mHsp60_{14}$–$(mHsp10_7)_2$ complex. (*A*) View from the north pole of the two mHsp60 rings. Blue circles represent the seven subunits of the north ring, and red circles represent the seven subunits of the south ring. Subunits of the north ring are named alphabetically from A to G, and subunits of the south ring are named alphabetically from H to N. The black line represents the twofold NCS symmetry axis. Views from the north pole of mHsp60–mHsp10 layout in the north ring (*B*) and in the south ring (*C*) are shown. Solid circles represent mHsp60 subunits. Dashed circles represent mHsp10 subunits. Filled small circles represent the approximate locations of the mobile loop of each mHsp10 subunit. The mHsp10 subunits are named alphabetically from O to U in the north ring and alphabetically/numerically from V to 2 in the south ring.

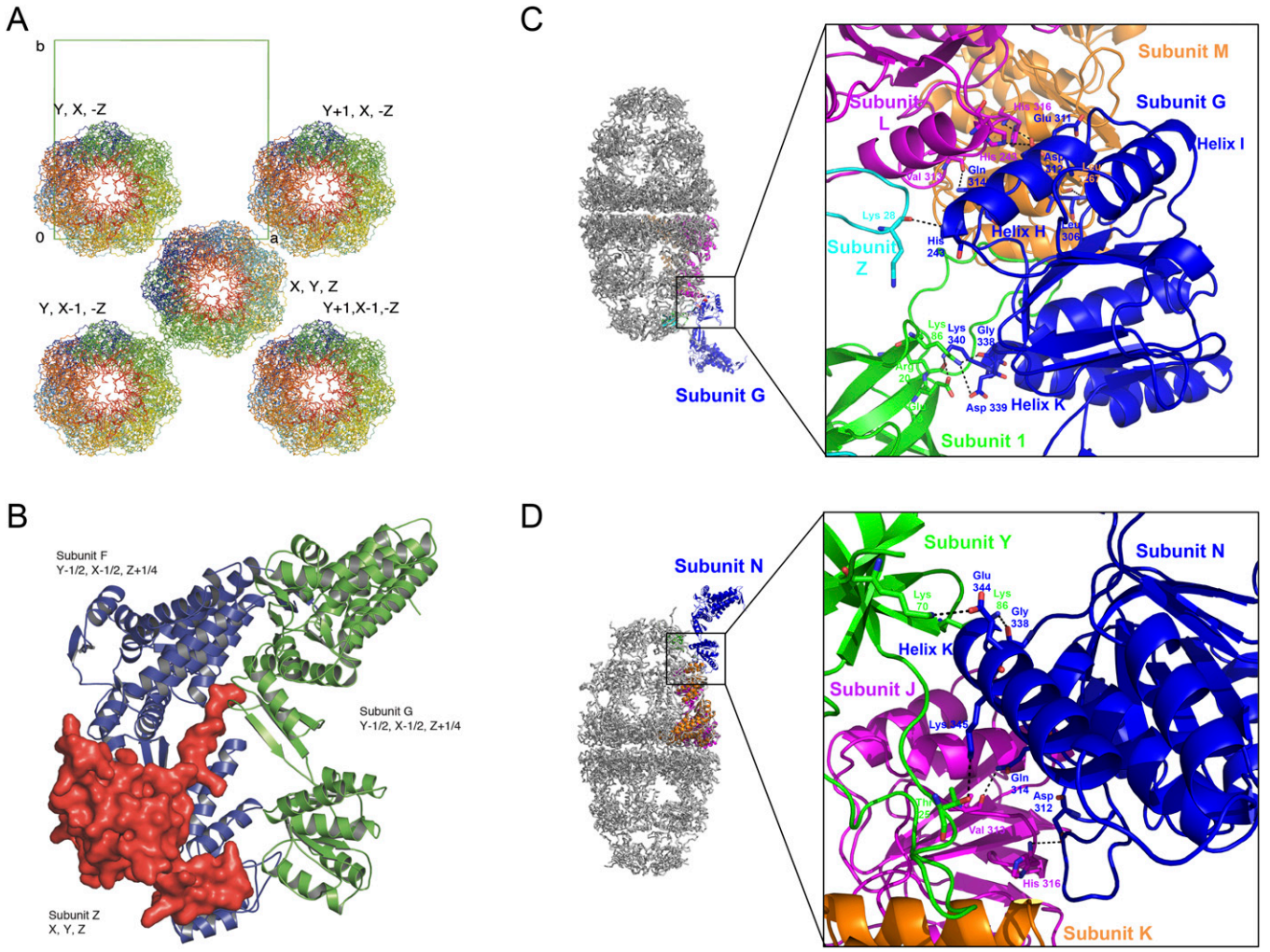

Fig. S5. Packing and stabilizing effect of the crystal lattice. (*A*) Four of the 12 packing neighbors in the equatorial plane of the mHsp60–mHsp10 complex with symmetry elements annotated. Disharmony between noncrystallographic sevenfold symmetry of the complex and crystallographic fourfold symmetry is clearly visible. (*B*) Insertion of the C-terminal His-tag region (visible on electron density map up to the first His residue His-110) of mHsp10, subunit Z (red surface), into a groove between symmetry-related subunits F and G of mHsp60 (blue and green ribbons, respectively). Symmetry elements and subunit names are annotated. (*C*) Lattice interactions of subunit G with subunits L, M, Z, and 1 in the symmetry-related football complex. A zoom-in view of the boxed area is presented. Subunit G is colored blue, L is colored magenta, M is colored orange, Z is colored cyan, and 1 is colored green. Interacting residues are labeled and presented as sticks. Bonds are indicated by black dashed lines. (*D*) Same as *C*, but for subunit N. Subunit N interacts with subunits J (magenta), K (orange), and Y (green) in the symmetry-related football complex.

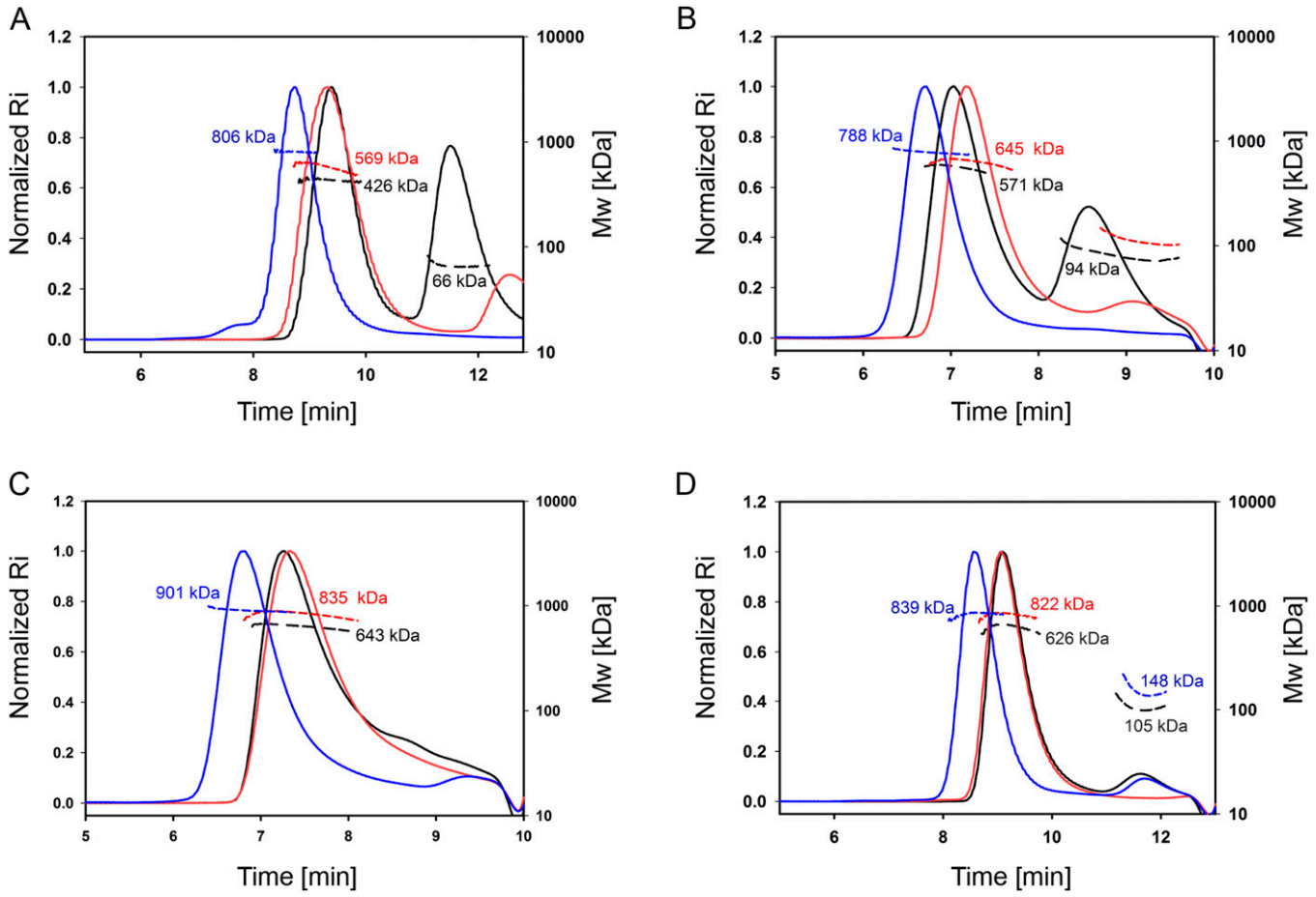

Fig. S6. SEC-MALS analysis of GroEL, WT mHsp60, and mHsp60^{E321K} mutant. WT mHsp60 is found in equilibrium between one and two rings, whereas the mHsp60 mutant adopts mainly a double-ring assembly. (*A*) Sec-MALS profiles of 50 μM GroEL (blue), WT mHsp60 (black), and mHsp60^{E321K} (red). Elution SEC profiles (solid lines) are plotted against the normalized refracting index (Ri) and the expected molecular mass (dashed lines). Average molecular mass values of the peaks are indicated. (*B*) Same as *A*, except that the proteins were incubated with 2 mM ATP for 5 min (the working buffer also contained 2 mM ATP). (*C*) Same as *B*, except that the proteins were incubated for 5 min with 50 μM 6× His-tagged mHsp10 (the same as the one used in the crystallization trials). (*D*) Same as *B*, except that the proteins were incubated for 5 min with 50 μM untagged mHsp10.

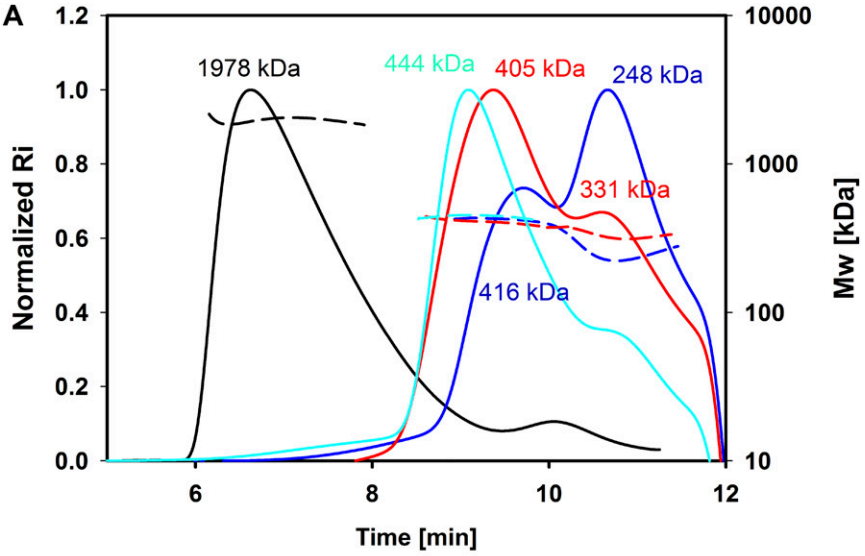

	Average molecular weight of the peak (kDa)
mHsp60^{TM} without ATP	1978
mHsp60^{TM} with ATP	416 (248 for second peak)
mHsp60^{TM} with His-tagged mHsp10 and ATP	405 (331 for second peak)
mHsp60^{TM} with untagged mHsp10 and ATP	444

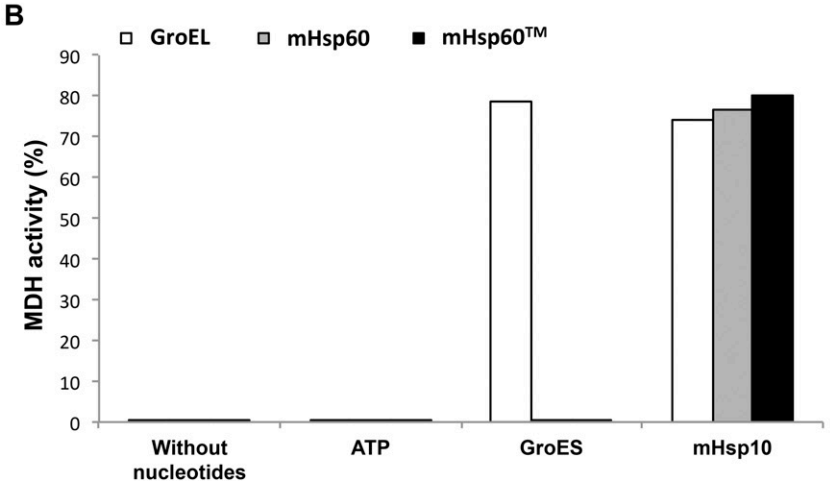

Fig. S7. mHsp60^{TM} mutant mainly forms single-ring complexes and is active in MDH refolding. (*A*) SEC-MALS analysis of mHsp60 (mutated in E105A, K109Q, and E462A). Different SEC-MALS profiles of 50 μM mHsp60 in diverse conditions are presented: without nucleotides (black), with 2 mM ATP (blue), with 50 μM His-tagged mHsp10 and 2 mM ATP (red), and with 50 μM untagged mHsp10 and 2 mM ATP (magenta). Elution SEC profiles (solid lines) are plotted against the normalized refracting index and the expected molecular mass (dashed lines). Average molecular mass values of the peaks are indicated above the peaks and are summarized in the table below the chart. (*B*) Refolding of 0.33 μM HCl-denatured MDH by 10 μM GroEL (white column), mHsp60 (gray column), or mHsp60^{TM} (black column) with buffer lacking nucleotides, buffer with 1 mM ATP, or buffer containing 20 μM mHsp10 or GroES and 1 mM ATP. MDH activity was measured at 340 nm after incubation for 60 min at 30 °C. The refolding activity is presented relative to the refolding activity of native MDH (100%).

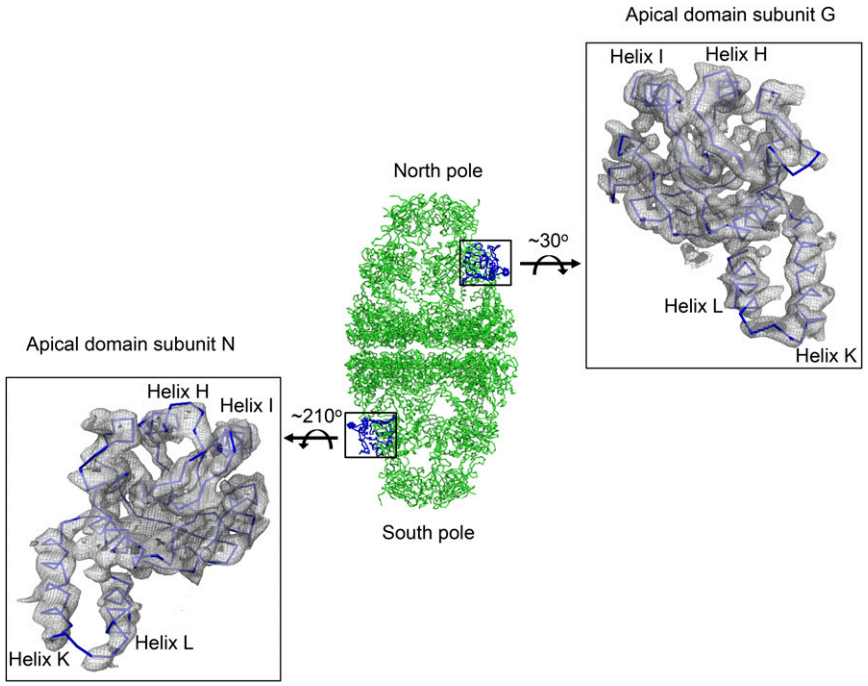

Fig. S8. Difference omit map of G and N subunit apical domains. A full side view of the football model (center) is presented here as a green ribbon. The apical domains of subunits G and N are presented as blue ribbons. On either side of the football model, a zoom-in view to the apical domains of subunits G and N is shown (boxed area in mHsp60 model). A F_o-F_c omit electron density map of the two apical domains is shown. The map was calculated by omitting the apical domains in subunits G and N from the final model and performing five cycles of refinement using REFMAC [version 5.7.32 (1)]. The map clearly indicates the trace of the apical domains of subunits G and N, thus verifying their atypical orientation. The difference map was calculated at a resolution range of 50–3.15 Å and contoured at a 2σ cutoff.

1. Murshudov GN, et al. (2011) REFMAC5 for the refinement of macromolecular crystal structures. *Acta Crystallogr D Biol Crystallogr* 67(Pt 4):355–367.

Table S1. Data collection and refinement statistics (molecular replacement)

Parameters	Native mHsp60–mHsp10 complex	$mHsp60^{Se\text{-}Met}$–mHsp10 complex*
Data collection		
Space group	$P4_12_12$	$P4_12_12$
Cell dimensions		
a = *b*, *c*; Å	199.10, 627.30	198.9, 629.8
a, *b*, *c*; °	90.0, 90.0, 90.0	90.0, 90.0, 90.0
Resolution, Å	49.77–3.15 (3.26–3.15)	42.20–3.80 (3.87–3.80)
R_{merge}†	0.14 (0.347)	0.105 (0.812)
I/σ(I)	9.0 (0.7)	9.2 (0.8)
Completeness, %	99.8 (99.1)	96.79 (60.0)
Redundancy	6.2 (4.1)	3.5 (4.4)
One-half set correlation CC(1/2) for the highest shell	0.382	0.423
Refinement		
Resolution, Å	49.78–3.15	
No. of reflections	215,814	
R_{work}/R_{free}	0.241/0.270	
No. of atoms	65,963	
Protein	65,571	
Ligand/ion	392	
Water	0	
B-factors (overall)	121.1	
Protein	120.60	
Ligand/ion	120.60	
Water	0	
rmsd		
Bond lengths, Å	0.004	
Bond angles, °	1.109	

Values in parentheses are for the shell with the highest resolution. Datasets were measured from one crystal.
*Dataset was used only for anomalous map calculation, and not for refinement.
†$R_{merge} = \sum_{hkl} \sum_i |I_i(hkl) - \langle I(hkl)\rangle| / \sum_{hkl} \sum_i I_i(hkl)$, where $\sum_{hkl}$ denotes the sum over all reflections and $\sum_i$ the sum over all equivalent and symmetry related reflections (1).

1. Stout GH, Jensen LH (1968) *X-Ray Structure Determination: A Practical Guide* (Macmillan, London).

Table S2. rmsd values of Cα (Å) between mHsp60 subunits

Subunit designation	Subunit designation													
	A	B	C	D	E	F	G	H	I	J	K	L	M	N
A		2.2	1.2	1	1.6	1.3	11	1.3	1.1	1.5	1.5	1.6	1.5	9.8
B			2	1.9	1.7	2.2	9.6	2.5	2.1	2.7	2.5	2.7	2.5	8.5
C				0.5	0.9	0.7	11.2	0.7	0.7	0.9	0.8	1.1	0.9	9.9
D					0.8	0.7	10.9	0.9	0.5	1.1	0.9	1.2	1	9.7
E						1	10.8	1.2	0.9	1.3	1.1	1.5	1.2	9.5
F							11.2	0.6	0.5	0.8	0.6	0.9	0.7	10
G								11.5	11	11.6	11.3	11.6	11.4	1.8
H									0.7	0.4	0.6	0.6	0.6	10.2
I										0.9	0.6	1	0.7	9.8
J											0.6	0.5	0.7	10.4
K												0.7	0.5	10.1
L													0.7	10.5
M														10.2
N														

Shaded boxes highlight the rmsd values of the asymmetric mHsp60 subunits G and N.

Table S3. rmsd values of Cα (Å) between mHsp10 subunits

Subunit designation	Subunit designation													
	O	P	Q	R	S	T	U	V	W	X	Y	Z	1	2
O		1	0.8	0.8	1	0.8	4.2	0.7	0.8	0.8	0.8	0.9	0.8	3.8
P			0.9	0.9	0.8	1.2	3.9	0.9	0.9	1.1	0.8	1.8	0.9	3.5
Q				0.6	0.8	0.6	4.4	0.7	0.6	0.7	0.8	0.8	0.6	4
R					0.9	0.7	4.4	0.7	0.6	0.7	0.8	0.7	0.7	3.8
S						0.9	4	0.6	0.7	0.9	0.8	0.8	0.8	3.3
T							4.5	0.7	0.7	0.6	0.8	0.8	0.6	3.8
U								4.2	4.3	4.4	4.3	4.2	4.3	1.2
V									0.6	0.6	0.7	0.7	0.6	3.8
W										0.7	0.7	0.7	0.5	3.8
X											0.7	0.8	0.5	3.9
Y												0.8	0.7	3.8
Z													0.7	4.1
1														3.8
2														

Shaded boxes highlight the rmsd values of the asymmetric mHsp10 subunits U and 2.